

# Orbital Interactions in the Ruthenium Olefin Metathesis Catalysts

Cherumuttathu H. Suresh<sup>\*,†</sup> and Nobuaki Koga<sup>\*,‡</sup>

Nagoya University Venture Business Laboratory and Graduate School of Information Science,  
Nagoya University, Chikusa-ku, Nagoya 464-8601, Japan

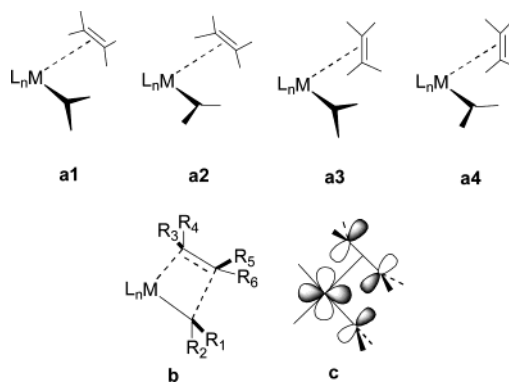
Received July 2, 2003

The structural and bonding interactions of the ruthenacyclobutane **4** suggested its nonclassical nature. A strong bonding interaction between the orbitals of the  $-\text{CH}_2\text{CH}_2-\text{CH}_2-$  fragment and the  $d_{yz}$  orbital on the metal in **4** was found that indicated the presence of two  $\alpha$ -CC agostic interactions in the complex. Further, in the transition state corresponding to the rate-determining step of the metathesis, mutually benefiting  $\pi$  interactions exist between the  $\text{Ru}=\text{CH}_2$  and the olefin fragments. These features are important in the metathesis activity of Grubbs first-generation catalyst because they make the potential energy surface of the  $\text{M}(\text{=CH}_2)(\text{C}_2\text{H}_4) \leftrightarrow \text{M}(\text{C}_2\text{H}_4)(\text{=CH}_2)$  region flat.

## Introduction

Well-defined ruthenium carbene complexes of the type  $(\text{PCy}_3)_2\text{Ru}(\text{CHR})\text{Cl}_2$  first introduced by Grubbs et al.<sup>1</sup> are highly active single-component (pre)catalysts for various types of alkene metathesis reactions such as ring-opening metathesis (ROM), ring-closing metathesis (RCM), ring-opening metathesis polymerization (ROMP), acyclic diene metathesis polymerization (ADMET), and cross-metathesis (CM).<sup>2</sup> There are several accounts in the literature on many exciting new developments in this field of research.<sup>3</sup> The generally accepted Hérisson–Chauvin mechanism (Scheme 1) contains the gist of the olefin metathesis mechanism,<sup>4</sup> which is described as a series of formal [2+2] cycloadditions and cycloreversions. A decade ago Eisenstein, Hoffmann, and Rossi had sketched out some interesting electronic features of the intermediate stages of olefin metathesis based on extended Hückel calculations.<sup>5</sup> They have pointed out that at first the attainment of the proper conformation of the olefin with respect to the carbene ligand is crucial for the catalytic activity. For instance, only conformation **a1** is productive in metathesis and **a2–a4** are not. Second, the olefin–metal–carbene complex or the metallacyclobutane (both in Scheme 1) may not be the stable geometry, but instead an intermediate nonclas-

sical structure **b** could be. Third, they suggest the orbital picture in the “collinear” conformation **c = a1** that maximizes the  $\pi$  bonding around a  $d^6$  octahedral metal center as the driving force for the metathesis.



We note that none of the previous DFT studies as well as experimental studies<sup>6–11</sup> have looked at the orbital interaction especially in the metallacyclobutanes that was pointed out by Hoffman and co-workers.<sup>5</sup> In the present work we undertake such a study on the orbital interactions that would govern the metathesis route. This study is expected to give more insights into the ruthenium olefin metathesis catalysts in general. Ac-

\* Corresponding authors. E-mail: suresh@info.human.nagoya-u.ac.jp; koga@is.nagoya-u.ac.jp.

<sup>†</sup> Nagoya University Venture Business Laboratory.

<sup>‡</sup> Graduate School of Information Science.

(1) (a) Nguyen, S. T.; Johnson, L. K.; Grubbs, R. H.; Ziller, J. W. *J. Am. Chem. Soc.* **1992**, *114*, 3974. (b) Schwab, P.; Grubbs, R. H.; Ziller, J. W. *J. Am. Chem. Soc.* **1996**, *118*, 100. (c) Dias, E. L.; Nguyen, S.-B. T.; Grubbs, R. H. *J. Am. Chem. Soc.* **1997**, *119*, 3887. (d) Ulman, M.; Grubbs, R. H. *Organometallics* **1998**, *17*, 2484. (e) Sanford, M. S.; Love, J. A.; Grubbs, R. H. *J. Am. Chem. Soc.* **2001**, *123*, 6543.

(2) (a) Ivin, K. J.; Mol, J. C. *Olefin Metathesis and Metathesis Polymerization*; Academic Press: San Diego, 1997. (b) Dörwald, F. Z. *Metal Carbenes in Organic Synthesis*; Wiley-VCH: Weinheim, Germany, 1999.

(3) (a) Frustner, A. *Angew. Chem., Int. Ed.* **2000**, *39*, 3012, and references therein. (b) Trnka, T. M.; Grubbs, R. H. *Acc. Chem. Res.* **2001**, *34*, 18.

(4) Hérisson, J.-L.; Chauvin, Y. *Makromol. Chem.* **1970**, *141*, 161.

(5) Eisenstein, O.; Hoffmann, R.; Rossi, A. R. *J. Am. Chem. Soc.* **1981**, *103*, 5582.

(6) (a) Hinderling, C.; Adlhart, C.; Chen, P. *Angew. Chem.* **1998**, *110*, 2831. (b) Tallarico, J. A.; Bonitatebus, P. J.; Snapper, M. L. *J. Am. Chem. Soc.* **1997**, *119*, 7157. (c) Kingsbury, J. S.; Harrity, J. P. A.; Bonitatebus, P. J.; Hoveyada, A. H. *J. Am. Chem. Soc.* **1999**, *121*, 791. (d) Dias, E. L.; Grubbs, R. H. *Organometallics* **1998**, *17*, 2758. (e) Sanford, M. S.; Henling, L. M.; Grubbs, R. H. *Organometallics* **1998**, *17*, 5384.

(7) (a) Adlhart, C.; Volland, M. A. O.; Hofmann, P.; Chen, P. *Helv. Chim. Acta* **2000**, *83*, 3306. (b) Adlhart, C.; Chen, P. *Helv. Chim. Acta* **2000**, *83*, 2192. (c) Hinderling, C.; Adlhart, P.; Chen, P. *Angew. Chem.* **1998**, *110*, 2831.

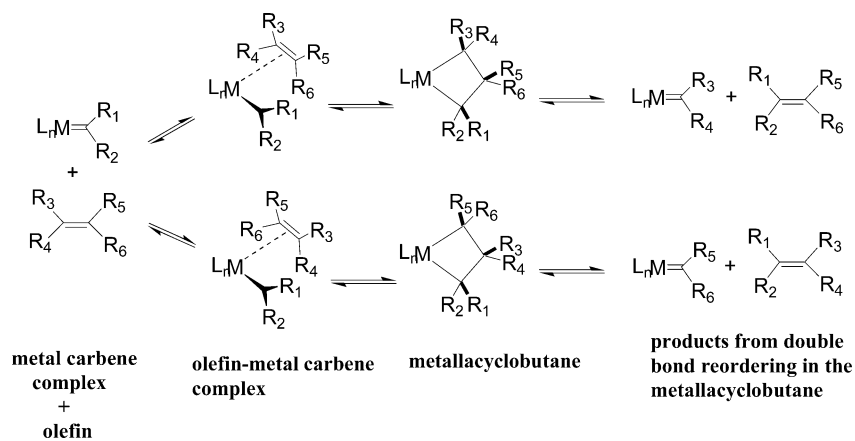
(8) Aagaard, O. M.; Meier, R. J.; Buda, F. *J. Am. Chem. Soc.* **1998**, *120*, 7174.

(9) Adlhart, C.; Hinderling, C.; Baumann, H.; Chen, P. *J. Am. Chem. Soc.* **2000**, *122*, 8204.

(10) (a) Cavallo, L. *J. Am. Chem. Soc.* **2002**, *124*, 8965. (b) Fomine, S.; Vargas, S. M.; Tlenkopatchev, M. A. *Organometallics* **2003**, *22*, 93.

(11) Vyboishchikov, S. F.; Buhl, M.; Thiel, W. *Chem. Eur. J.* **2002**, *8*, 3962.

## Scheme 1. Generalized Hérisson–Chauvin Mechanism of Olefin Metathesis



## Scheme 2. Generally Accepted Mechanism of Ruthenium-Catalyzed Olefin Metathesis

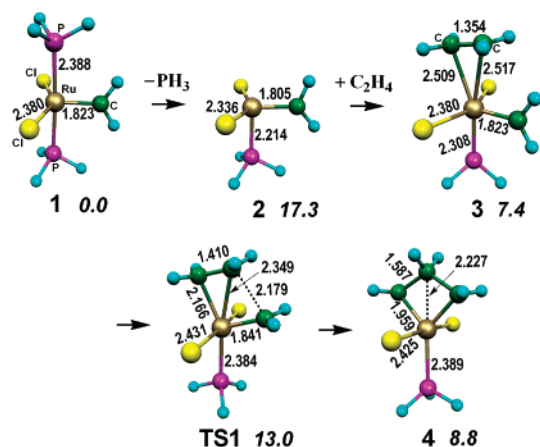
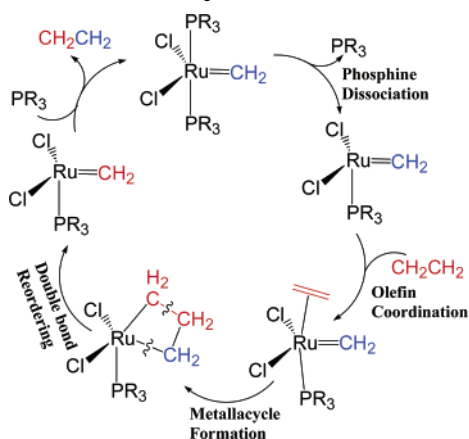


**Figure 1.** Generally accepted mechanism for ruthenium olefin metathesis. The values in italics correspond to relative values of enthalpy in kcal/mol. Bond lengths are in angstroms.

cordingly, we conduct this study on the olefin metathesis of ethene with the model bisphosphine complex  $(\text{PH}_3)_2\text{-Ru}(\text{CH}_2)\text{Cl}_2$ , **1**.

## Computational Methods

All the molecular geometries were optimized at the DFT level of theory using the B3LYP hybrid functional<sup>12</sup> with the Gaussian 98 suite of programs.<sup>13</sup> For Ru, the basis set LanL2DZ with extra f-polarization functions was used.<sup>14</sup> In this basis set the 28 innermost electrons of Ru have been replaced by a relativistic core potential (ECP) of Hay and Wadt.<sup>15</sup> For H and C, 6-31G\*\* and for P and Cl, 6-31+G\* basis

sets were selected.<sup>16</sup> This method abbreviated here as B3LYP/BI would give reliable geometries.<sup>17</sup> Normal coordinate analysis has been performed for all stationary points to characterize the transition states (TSs) and equilibrium structures.

## Results and Discussion

The mechanism depicted in Scheme 2 has emerged as the most reliable mechanism for the olefin metathesis reaction, as confirmed from the recent experimental and theoretical works.<sup>6–11</sup> The various steps of this mechanism include (i) dissociation of one of the phosphine ligands from the bisphosphine complex followed by (ii) coordination of the olefin to ruthenium that results in (iii) the formation of a ruthenium metallacycle and then (iv) the double-bond reordering leading to the product. In the present study, we have calculated the potential energy diagram corresponding to this particular mechanism at the B3LYP/BI level of theory, which is depicted in Figure 1 along with the respective geometries.

In this mechanism, the phosphine dissociation from  $\text{RuCl}_2(\text{CH}_2)(\text{PH}_3)_2$  (**1**) is endothermic by 17.3 kcal/mol. The monophosphine complex **2** thus generated is a 14-electron species with four ligands, and it could have an

(12) (a) Becke, A. D. *J. Chem. Phys.* **1993**, *98*, 1372. (b) Becke, A. D. *J. Chem. Phys.* **1993**, *96*, 5648.

(13) Frisch, M. J.; Trucks, G. W.; Schlegel, H. B.; Scuseria, G. E.; Robb, M. A.; Cheeseman, J. R.; Zakrzewski, V. G.; Montgomery, Jr., J. A.; Stratmann, R. E.; Burant, J. C.; Dapprich, S.; Millam, J. M.; Daniels, A. D.; Kudin, K. N.; Strain, M. C.; Farkas, O.; Tomasi, J.; Barone, V.; Cossi, M.; Cammi, R.; Mennucci, B.; Pomelli, C.; Adamo, C.; Clifford, S.; Ochterski, J.; Petersson, G. A.; Ayala, P. Y.; Cui, Q.; Morokuma, K.; Malick, D. K.; Rabuck, A. D.; Raghavachari, K.; Foresman, J. B.; Cioslowski, J.; Ortiz, J. V.; Stefanov, B. B.; Liu, G.; Liashenko, A.; Piskorz, P.; Komaromi, I.; Gomperts, R.; Martin, R. L.; Fox, D. J.; Keith, T.; Al-Laham, M. A.; Peng, C. Y.; Nanayakkara, A.; Gonzalez, C.; Challacombe, M.; Gill, P. M. W.; Johnson, B.; Chen, W.; Wong, M. W.; Andres, J. L.; Gonzalez, C.; Head-Gordon, M.; Replogle, E. S.; Pople, J. A. *Gaussian 98, Revision A.11*; Gaussian, Inc.: Pittsburgh, PA, 1998.

(14) f-Polarization functions are taken from: Ehlers, A. W.; Bohme, M.; Dapprich, S.; Gobbi, A.; Hollwarth, A.; Jonas, V.; Kohler, K. F.; Stegmann, R.; Veldkamp, A.; Frenking, G. *Chem. Phys. Lett.* **1993**, *208*, 111.

(15) (a) Hay, P. J.; Wadt, W. R. *J. Chem. Phys.* **1985**, *82*, 275. (b) Wadt, W. R.; Hay, P. J. *J. Chem. Phys.* **1985**, *82*, 284. (c) Hay, P. J.; Wadt, W. R. *J. Chem. Phys.* **1985**, *82*, 299.

(16) Hariharan, P. C.; Pople, J. A. *Mol. Phys.* **1974**, *27*, 209.

(17) Foresman, J. B.; Frisch, A. E. *Exploring Chemistry with Electronic Structure Methods*, 2nd ed.; Gaussian Inc.: Pittsburgh, PA, 1995; Chapter 7, p 158.

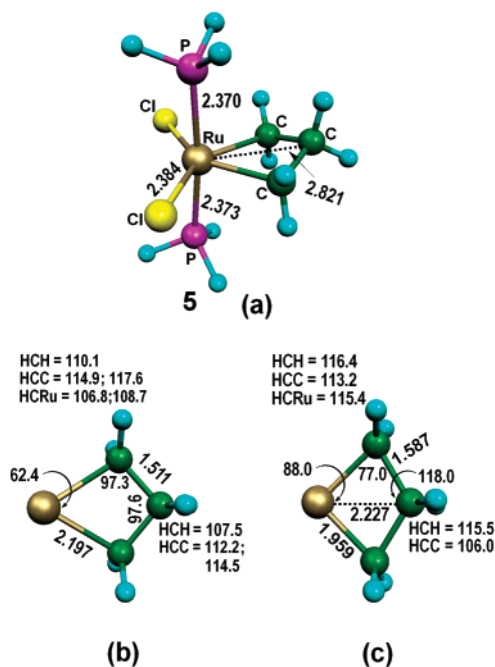


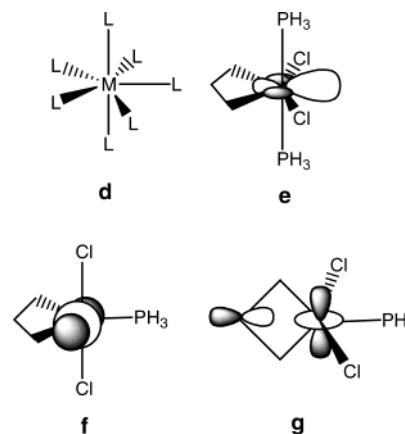
**Figure 2.** (a) Structure of bisphosphine ruthenacyclobutane complex **5**, (b) metallacyclobutane region of **5**, and (c) metallacyclobutane region of **4**. The depicted bond length and bond angle values are in angstroms and degrees, respectively.

open shell electronic structure. However, there was no inherent instability in the closed shell electronic structure of **2**, as it was verified from the stability test calculation.<sup>18</sup> The incoming ethene then coordinates to the monophosphine complex (**2**) so that it is trans to the phosphine ligand. This step producing **3** is a barrierless process. The formation of ruthenacyclobutane starts from this 16-electron intermediate **3** as it passes through the four-centered **TS1**. In **TS1**, the length of the newly forming CC bond is 2.179 Å, which is still 1.373 times longer than the CC bond in the product **4** of this step. The  $\pi$  orbital of methylene of **TS1** is directed toward the ethene, and therefore the new CC bond formation is expected to be easy.<sup>19</sup> The low activation enthalpy of 5.6 kcal/mol also supports the early formation of **TS1**. For the reverse reaction corresponding to the double-bond reordering, viz., **4**  $\rightarrow$  **TS1**  $\rightarrow$  **3**, requires an activation enthalpy of only 4.2 kcal/mol. These B3LYP calculation results reproduced those of previous theoretical studies.<sup>10,11</sup> During the reaction from **3** to **4**, the Ru atom is formally oxidized to Ru(IV). At the four-membered ruthenacyclobutane ring of the electron-deficient 14-electron five-coordinate complex **4**, interesting structural features as described below are observed (cf. Figure 2).<sup>5</sup>

The CC bond lengths of 1.587 Å are much longer than the typical CC single-bond length, and the distance of 2.227 Å between the Ru atom and the central carbon atom is close to that of 1.959 Å between the Ru atom and the terminal carbon atoms. The latter leads to considerable deviation of the CCRu (77.0°) and CCC

(118.9°) bond angles from the CCC bond angle of 90° in the case of cyclobutane as an ideal situation for a four-membered ring. In other words, we can say that ruthenacyclobutane **4** has a nonclassical structure. These structural features suggest that the CCC fragment of **4** interacts strongly with the Ru atom via one of the vacant d orbitals of Ru. This point of view became clearer when we found that a bisphosphine ruthenium complex **5** reported in the work of Thiel et al.<sup>11</sup> has a classic structure. The geometry of **5** obtained using the present method is depicted in Figure 2. As we can see, unlike **4**, apparently there is no bonding interaction in **5** between C<sub>(middle)</sub> and Ru atoms. More on the interaction between the CCC fragment and the Ru atom will be discussed in the next section to clarify the character and role of this interaction.

Comparison of the structures between **4** and **5** shows other structural features in **4**. While the HCH angles of all methylene groups and the HCRu angles of the terminal methylene groups in **5** are close to 110° expected for sp<sup>3</sup> carbon atoms, those in **4** are larger, pointing out the significant deviation of carbon centers from the sp<sup>3</sup> hybridization. This suggests that methylene groups possess some amount of carbene-like character in **4**.



**Intramolecular Interactions in the Ruthenacyclobutane Intermediate.** In Figure 3, the important orbitals<sup>20</sup> corresponding to the CC bonds of cyclobutane and the CC and RuC bonds of **4** and **5** are depicted. Ruthenacyclobutane **5** is a six-coordinate 16-electron complex with the d<sup>4</sup> Ru atom. While seven-coordinate 18-electron complex ML<sub>7</sub> as shown in **d** is known, **5** is regarded as the complex directly formed by the dissociation of one of the equatorial ligands from ML<sub>7</sub>. Consequently, in **5** the vacant orbital extends toward the vacant coordination site as shown in **e**. Further, in **5** the nodal properties of the occupied molecular orbitals (MOs) representing the bonds of the ruthenacyclobutane moiety are similar to those of the CC bonds of cyclobutane, reflecting the structure of the classical metallacyclobutane (cf. Figure 3). On the other hand, in **4**, the d<sub>z<sup>2</sup></sub> orbital shown in **f** is formally empty. The middle carbon (C<sub>(middle)</sub>) interacts with this vacant orbital as

(18) See also: (a) Seeger, R.; Pople, J. A. *J. Chem. Phys.* **1977**, *66*, 3045. (b) Bauernschmitt, R.; Ahlrichs, R. *J. Chem. Phys.* **1996**, *104*, 9047. (c) Schlegel, H. B.; McDouall, J. J. In *Computational Advances in Organic Chemistry*; Ogretir, C., Csizmadia, J. G., Eds.; Kluwer Academic: The Netherlands, 1997; p 167.

(19) Upton, T. H.; Rappé, A. K. *J. Am. Chem. Soc.* **1985**, *107*, 1206.

(20) For the visualization of molecules and orbitals see: (a) Flükiger, P. F. Development of the molecular graphics package MOLEKEL and its application to selected problems in organic and organometallic chemistry. Thèse No. 2561, Département de Chimie Physique, Université de Genève, Genève, 1992. (b) Portmann, S.; Lüthi, H. P. *CHIMIA* **2000**, *54*, 766.

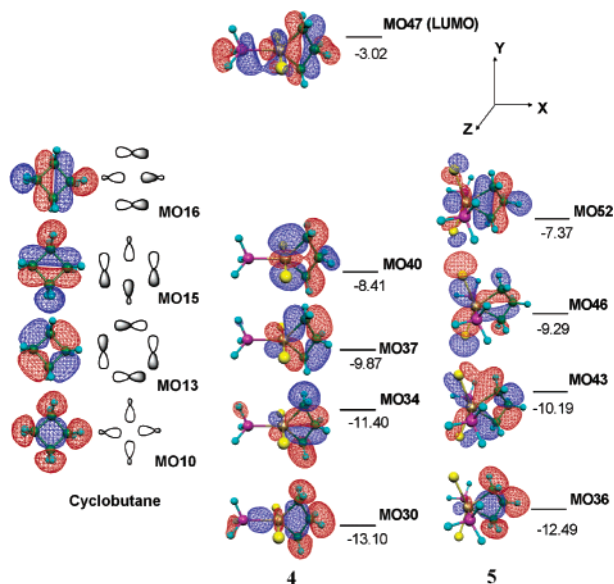


**Figure 3.** Occupied MOs that describe the CC bonds of cyclobutane and the CC and RuC bonds of ruthenacyclobutanes **4** and **5** (MO energies in eV). MO similar to MO16 of cyclobutane is a LUMO in **4**. There is a bonding interaction between CCC and  $d_{yz}$  in MO40 of **4**.

shown in **g** to deform the CCC fragment. One can find such an interaction in MO40 of **4** as shown in Figure 3. It corresponds to the interaction between the CCC bonding orbital and the empty  $d_{yz}$  orbital. As a result of this interaction, the MOs of **4** representing the bonds of the four-membered ring are quite different in nature from those of CB as well as **5**. Three low-lying occupied orbitals of **4**, viz., MOs 30, 34, and 37, are similar to the MOs 10, 15, and 13 of CB, respectively, whereas the MO of **4**, similar to the occupied MO16 of CB with the out-of-phase mixing between two diagonal carbons, is vacant (LUMO) and instead the MO40 is occupied. Thus, the bonding and the structural features are nonclassical for **4**.

The interaction between the ruthenium  $d_{yz}$  orbital and the CCC bonding orbital is equivalent to two  $\alpha$ -CC agostic interactions.<sup>21</sup> As found in the case of the agostic interaction, this type of interaction could make the CC bond cleavage easy.<sup>21b</sup> This can be considered to be an important effect of the Grubbs catalyst.

**Orbital Interactions in TS1.** Although there are several paths described in the recent theoretical calculations, what makes the metathesis path in Figure 1 the most important? In this mechanism, **TS1** corresponds to the transition state of the rate-determining step. This TS has a structure very similar to that proposed by Hoffmann and co-workers (structure **b**).<sup>5</sup> However, contrary to their proposal, **TS1** is a transition state and the metallacyclobutane structure **4** is a minimum energy conformation. To understand the low barrier of the rate-determining step of this mechanism, we have analyzed the orbital interactions between ethene and the Ru=CH<sub>2</sub> fragment in **TS1**. The com-

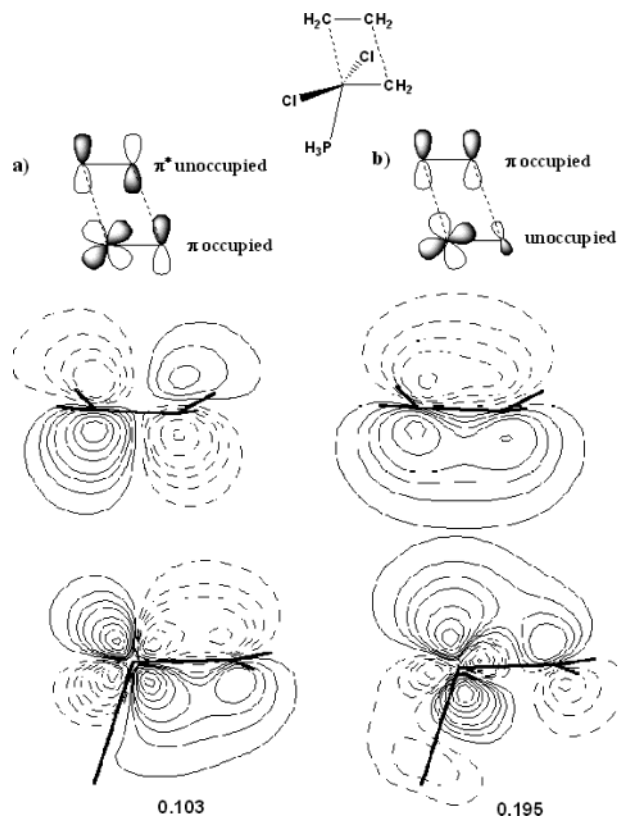


**Figure 4.** Pairs of fragment orbitals representing the interaction (a) between the occupied orbitals of (PH<sub>3</sub>)Cl<sub>2</sub>Ru=CH<sub>2</sub> and the unoccupied orbitals of C<sub>2</sub>H<sub>4</sub> and (b) between the unoccupied orbitals of (PH<sub>3</sub>)Cl<sub>2</sub>Ru=CH<sub>2</sub> and the occupied orbitals of C<sub>2</sub>H<sub>4</sub>. The depicted numbers are the Mulliken overlap population between fragment orbitals.

puted fragment orbitals<sup>22</sup> of **TS1** are shown in Figure 4 along with their schematic representations. As it can be seen from this figure, the occupied  $\pi$  orbital of the Ru=CH<sub>2</sub> bond interacts strongly with the unoccupied  $\pi^*$  orbital of the CH<sub>2</sub>CH<sub>2</sub> fragment (Mulliken overlap population = 0.103), and at the same time the unoccupied orbital consisting of the  $\pi^*$  orbital of the Ru=CH<sub>2</sub> bond and the unoccupied d orbital overlaps well with the  $\pi$  occupied orbital of the CH<sub>2</sub>CH<sub>2</sub> fragment (Mulliken overlap population = 0.195). Of these two interactions, the former is the same as that in **c**.<sup>5</sup> These mutually benefiting  $\pi$  interactions and the CC agostic interaction found in **4** can be considered as the main driving force for the metallacyclobutane formation and the easy double-bond reordering in the metathesis reactions. In other words, the potential energy surface corresponding to the **3**  $\rightarrow$  **TS1**  $\rightarrow$  **4**  $\rightarrow$  **TS1**  $\rightarrow$  **3** region becomes flat due to these interactions, and it makes the olefin metathesis a facile process.

**Importance of CC Agostic Interaction.** Well-characterized CC agostic complexes are very rare as compared to the  $\alpha$ -C-H and  $\beta$ -C-H agostic complexes.<sup>21</sup> However, there is growing evidence indicating that CC bonds can also participate in agostic interactions that lead to important chemical transformations. A good example of such bonding is described in the very recent work of Maseras et al.,<sup>23</sup> as they presented structural, spectroscopic, and theoretical evidence for an unprec-

(21) (a) Brookhart, M.; Green, M. L. H. *J. Organomet. Chem.* **1983**, *250*, 395. (b) Koga, N.; Obara, S.; Kitaura, K.; Morokuma, K. *J. Am. Chem. Soc.* **1985**, *107*, 7109. (c) Koga, N.; Obara, S.; Morokuma, K. *J. Am. Chem. Soc.* **1984**, *106*, 4625. (d) Obara, S.; Koga, N.; Morokuma, K. *J. Organomet. Chem.* **1984**, *270*, C33. (e) Koga, N.; Morokuma, K. *J. Am. Chem. Soc.* **1988**, *110*, 108. (f) Suresh, C. H.; Koga, N. *Organometallics* **2001**, *20*, 4333.

(22) Fujimoto, H.; Koga, N.; Fukui, K. *J. Am. Chem. Soc.* **1981**, *103*, 7452.

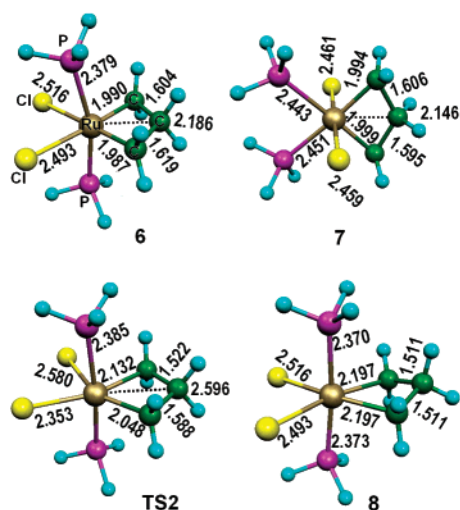


**Figure 5.** Optimized geometries of CC agostic complexes **6** and **7**, transition state **TS2**, and **8**. The relative potential energies of **6**, **7**, and **TS2** are 13.2, 8.3, and 22.8 kcal/mol higher than that of structure **5** depicted in Figure 2. **TS2** is located between **5** and **6**. See text for more details.

edented CC agostic interaction in a cyclopropyl tris-(pyrazolyl)boratoniobium complex. We have already reported that in the ruthenacyclobutane bisphosphine complex **5** depicted in Figure 2 there is no CC agostic interaction. However, two other possibilities of ruthenacyclobutane bisphosphine complexes recently appearing in the literature are interesting. The first one (structure **6**) is described in the associative metathesis path obtained by Thiel et al.,<sup>11</sup> and the second one (structure **7**) is found in the very recent work of Bernardi et al.<sup>24</sup> The structures of **6** and **7** obtained from the present level of calculations (cf. Figure 5) are 13.2 and 8.3 kcal/mol, respectively, less stable than complex **5**. Though nothing was written on the agostic character of **6** and **7** in previous works,<sup>11,24</sup> we can see that both of them are CC agostic complexes because their CC bonds are elongated to a significant extent as compared to a typical CC single bond and the RuC<sub>(middle)</sub> distance is quite similar to the other two RuC bond lengths. Further, the orbital analysis of **6** and **7** showed the presence of the agostic bonding orbital similar to the one we have found for complex **4**. Thus the CC agostic interaction can be considered as an important feature of both the dissociative and associative pathways of

ruthenium olefin metathesis reactions. It is to be noted that the two CC bonds in **4**, **6**, and **7** are  $\alpha$ -CC bonds, and therefore these complexes are characterized by the presence of two agostic  $\alpha$ -CC bonding interactions, a unique feature not often observed in other transition metal complexes. We have also located a transition state, **TS2** (cf. Figure 5), that connects the agostic complex **6** and the nonagostic complex **5**. This particular transformation was not found in the associative reaction path described by Thiel et al.<sup>11</sup> According to them, the reaction step corresponding to the double-bond reordering of metathesis (cf. Scheme 1) would occur from the agostic complex **5**.

How do we obtain a reasonably good estimate of the strength of the  $\alpha$ -CC agostic interactions in **4**, **6**, and **7**? When **6** is changed to **5** via **TS2**, not only are the agostic interactions broken but also a significant change of the ClRuCl bond angle occurs (the ClRuCl angle of 85.3° in **6** is changed to 138.0° in **5**). Therefore, structure **8** is constructed, keeping the geometry parameters of the (PH<sub>3</sub>)<sub>2</sub>Ru(CH<sub>2</sub>CH<sub>2</sub>CH<sub>2</sub>) unit the same as that of **5** while its RuCl distances and ClRuCl and ClRuC<sub>(middle)</sub> angles are kept to the same values as those of **6**. Structure **8** is 17.7 kcal/mol higher in energy than **6**. This difference in energy mainly arises due to the absence of agostic interaction in **8**, and therefore we consider this value as an upper bound for the strength of  $\alpha$ -CC agostic interactions. Nearly the same amount of agostic interaction is expected in **4** and **7**. It is thus clear that the agostic interaction significantly stabilizes the ruthenacyclobutane intermediate. Further, it weakens both  $\alpha$ -CC bonds and thereby enhances the rupture of a CC bond toward the double-bond reordering process.

## Conclusions

The low barrier of the rate-determining step of the generally accepted metathesis path can be attributed to two main orbital interactions, viz., (i) the strong  $\pi$  orbital interactions between the Ru=CH<sub>2</sub> and the olefin moiety in **TS1** and (ii) the two  $\alpha$ -CC agostic orbital interactions in the metallacyclobutane **4**. These orbital interactions make the potential energy surface of (PH<sub>3</sub>)<sub>2</sub>RuCl<sub>2</sub>(=CH<sub>2</sub>)(C<sub>2</sub>H<sub>4</sub>)  $\leftrightarrow$  (PH<sub>3</sub>)<sub>2</sub>RuCl<sub>2</sub>(C<sub>2</sub>H<sub>4</sub>)(=CH<sub>2</sub>) flat, and therefore the metathesis reaction becomes a facile process. It is felt that the  $\alpha$ -CC agostic interaction is an important feature of the ruthenium olefin metathesis reactions.

**Acknowledgment.** Some of the calculations were carried out at the Research Center for Computational Science of Okazaki National Research Institutes, Japan.

OM034011N

(23) (a) Jaffart, J.; Etienne, M.; Reinhold, M.; McGrady, J. E.; Maseras, F. *Chem. Commun.* **2003**, 876. (b) See also: Ujaque, G.; Maseras, F.; Lledós, A.; Contreras, L.; Pizzano, A.; Rodewald, D.; Sánchez, L.; Carmona, E.; Monge, A.; Ruiz, C. *Organometallics* **1999**, *18*, 3294.

(24) Bernardi, F.; Bottoni, A.; Miscione, G. P. *Organometallics* **2003**, *22*, 940.